



On the Mechanical Behavior of Distinct Auto Wheel Materials Under Static and Dynamic In-service Loading Cycle

Aniekan Essienubong IKPE^{1*}, Emem Okon IKPE², Ekom Mike ETUK³

¹Department of Mechanical Engineering, University of Benin, PMB. 1154 Benin City, Nigeria

* **Corresponding Author** : aniekan.ikpe@eng.uniben.edu --ORCID: 0000-0001-9069-9676

²Department of Science Technology, Akwa Ibom State Polytechnic, Ikot Osurua, PMB 1200, Nigeria

ememohi83@yahoo.com --ORCID: 0000-0001-8093-9904

³Department of Production Engineering, University of Benin, PMB. 1154 Benin City, Nigeria

alwaysetuk@gmail.com --ORCID: 0000-0002-1866-9349

Article Info:

DOI: 10.22399/ijcesen.913166

Received : 11 April 2021

Accepted : 16 June 2021

Keywords

Auto wheel
Mechanical behaviour
Density
Failure
Static stress
Bending

Abstract:

Automobile wheels serve as a primary means of support to a moving and stationary car while being subjected to static and dynamic loading in the process. The present study examines the mechanical behavior of different auto wheel materials under the aforementioned loading conditions using Finite Element Method (FEM). The wheel component was modlled and simulated with SOLIDWORKS 2018 version using different materials including carbon fibre (T300), cast alloy steel, aluminium (2014-T6) and magnesium alloy. Considering the simulation constraints of lowest static stress (von-mises), lowest resultant strain, lowest displacement (static and raidal) and lowest bending, cast alloy steel met all the requirements except for static strain where carbon fibre was the lowest followed by cast alloy steel. Carbon fibre (T300) among all the materials had the highest static stress (von-mises), highest displacement (static and raidal) and highest bending. Static stress for aluminium (2014-T6) was lower than that of magnesium alloy while resultant strain, static and radial displacement as well as bending were lower for aluminium (2014-T6) than magnesium alloy. Von-mises stresses for all wheel materials where below their yield strength, indicating that they can perform optimally under the above mentioned loading constraints. The main disadvantage with steel wheel is the high density while low density of the other three materials offer a distinctive advantage to auto performance, but steel wheel is inexpensive, strong, tough and more durable compared to the other materials.

1. Introduction

A wheel is a circular-shaped structure designed with extreme toughness and high strength to withstand radial, tangential and axial forces it is exposed to when subjected to rotational motion. The centre of the wheel is bored of a circular hole were an axle bearing is tightened about to enable the wheel rotate when a moment generated by the auto engine is applied to the vehicle axle about its axis and the

wheel [1]. In other words, the wheel is one of the most important rotating circular member of a vehicle, upon which the tyre is installed in between the flange at a pressure (35-40 Psi) different from the ambient pressure [2, 3]. Automobile wheel assembly is one of the most important aspects that determine mobility in automotive applications and its failure can be hazardous if not properly engineered to bring out the best performance, strength, durability and reliability. The design of a wheel assembly is critical

due to the forces acting on it during acceleration, braking, cornering and tilting [4]. Weight, manufacturability, performance and aesthetics are the four essential technical factors considered in the design of auto wheel. It is usually designed to possess adequate strength to enable it perform the desired functions, should be balanced statically and dynamically as well, and should be produced from very light materials to reduce unsprung weight. Steel wheels are comparably stronger than wire and alloy wheels, but it is heavier than alloy wheels which increases the vehicle unsprung weight. On the other hand, alloy wheels are recommended for automobile applications because they reduce unsprung weight of the vehicle [5, 6]. Bisht and Awasthi [7] reported the percentage weight of different wheel types as follows: Steel wheel (100%), Wire wheel (85%), alloy wheel (75%) and composite wheel (60%). Nomenclature of a wheel-rim profile consist of the wheel (rim and disc forms wheel), Rim (a section of wheel that the tyre is installed), disc (a section of the wheel attached to the axle hub of the vehicle) as well as the bead seat (a section of the rim that holds the tyre in a radial direction and in contact with the bead face) [8, 9]. Depending on the purpose of design, loading conditions and material capacity to withstand severe loading conditions, automobile wheels can be classified. For example, heavy loading may require steel wheels (density: 7.8 g/cc) due to their strength while medium and low load condition may require aluminium alloys (density: 2.7 g/cc) and magnesium alloys (Density: 1.54 g/cc) [10]. Prasad et al. [11] employed CATIA 5R17 software in the modelling of aluminium alloy and forged steel wheel rims which were further imported to ANSYS software to simulate the forces, pressure (21.3kpa was applied along the circumference of each wheel rim) acting on them and their effects on the wheel rim. Static displacement, Von-mises stress, stress intensity and dynamic displacement were 4.1168e-6mm, 9.748e5 Mpa, 1.0611e6 Mpa and 0.71537 mm as well as 4.077e-6 mm, 3.2348e6 Mpa, 3.3759e6 Mpa and 0.43427 mm for aluminium alloy and forged steel wheel rims, making forged steel a better material for wheel design over aluminium alloy. Venkateswarlu and Sharma [12] designed and analysed three different alloy wheel materials including aluminium alloy, magnesium alloy and titanium alloy. The wheel was modelled with CATIA V5 R20 while simulation of the model was carried out with ANSYS workbench. Total deformation values obtained from the static analysis were 0.13156, 0.13505 and 0.16258 for aluminium alloy, magnesium alloy and titanium alloy. This indicates that aluminium alloy among the three materials will exhibit the least level of deformation under static condition. Kumar et al. [13] carried out

similar study on different alloy wheel materials (aluminium alloy, steel and magnesium alloy) using CATIA V5 for the modelling and ANSYS software for the simulation. Steel wheel exhibited the least level of deformation (0.00029 mm), followed by magnesium alloy (0.00072 mm) and aluminium alloy (0.001287 mm). Using ANSYS software, Burande and Kazi [14] modelled and simulated two aluminium alloy wheels (Aluminium A356.2 and Aluminium 7075-T6) for passenger car under radial load. Finite Element Analysis (FEA) was used in the simulation to determine the stress and displacement factors in service condition. Aluminium A356.2 yielded Von-mises stress of 43.95 MPa and displacement of 32.33 mm while Aluminium 7075-T6 yielded Von-mises stress of 35.75 MPa and displacement of 23.81 mm. The analysis indicated that Aluminium 7075-T6 has a higher fatigue life (1×10^6 cycles.) than aluminium A356.2 (7.9985×10^5 cycles). Sekhar and Mouli [15] examined the application of Finite Element Technique (FET) for analysing the stress and displacement distribution in AL2024-T351 and Al 2064-T6 alloy wheels under conjoint influence of inflation pressure and radial load. The deflection for AL2024-T351 alloy wheel was found to be 0.164 mm which is much lower than that of aluminum (Al 2064-T6) alloy wheel which was 0.285mm, indicating that AL2024-T351 is much stiffer than aluminum (Al 2064-T6) alloy wheel. Results from the static analysis revealed that maximum normal stress obtained from Al 2064-T6 alloy wheel was 78.6% higher than that of Al2024-T351 alloy wheel while the Von-mises stress obtained for Al 2064-T6 alloy wheel was 50% higher than that of Al2024-T351 alloy wheel. It was observed that the stress and displacement increased while the in-service life of the wheel decreased as the operational speed increased. In actual case scenario, determining the mechanical behaviour of auto wheels (as per the ISO 7141-Road Vehicles-Wheels-Impact Test Procedure, and SAE J175-Impact Test Procedure Standards) is important. However, testing and inspection procedure during development process of auto wheels are time consuming and expensive. Moreover, it is difficult to estimate the stress behaviour through theoretical approaches and elementary mechanical approximations. For these reasons, a 3D static analysis of any given auto wheel which involves complicated geometries and assumptions can be employed. The present study therefore involves determination of stresses, strains, displacements as well as bending induced on different auto wheel materials (designed with different materials) due to static and dynamic loads. The study involves Finite Element Modelling (FEM) of the auto wheel using SOLIDWORKS 2018 version and simulation of the

modelled component as well, in order to determine the mechanical behaviour of each material for auto wheel applications. For economic reasons, this can reduce the time, energy and resources involved in the development of prototype designs and testing phase of auto wheel.

2. Research Methodology

A given automotive wheel in motion is subjected to the following forces and moments: longitudinal force, lateral force (cornering force), vertical force (load), roll moment (overturning moment), pitch moment, yaw moment [16]. A given rotating vehicle wheel is subjected to radial loading due to pressure distribution which acts directly in the circumferential direction along the bead seat [17]. The pressure distribution is given by Equation 1. From Equation 1, radial load acting on a given car wheel can be determined using Equation 2:

$$W_r = W_0 * \cos\left(\frac{\pi}{2} * \frac{\theta}{\theta_0}\right) \quad (1a)$$

$$W_0 = \frac{W\pi}{br_b4\theta_0} \quad (1b)$$

$$F_r = 2b \int_{-\theta_0}^{\theta_0} W_n * r_b d\theta = 8 * b * r_b * \theta_0 * \frac{W_n}{\pi} \quad (2)$$

Where W_n is the natural frequency, W denotes the radial load, θ is the angle of loading, θ_0 is the angle at maximum load, F_r is the radial force, b is the width of the bead seat, r_b is the radius of the bead seat and W_r represents the pressure distribution. The wheel rolling radius can be determined as expressed in Equation 3 based on the relationship between the wheelset, wheel rotation and the formation of the traction force [18, 19]. On the other hand, Jazar [20] proposed the wheel rolling radius as expressed in Equation 4 while Wilson et al. [21] proposed the wheel rolling radius based on the function of drive torque, load, and pressure as given in Equation 5.

$$R_D = R_u - \rho_o \left[\text{Darctan}\left(B \frac{\rho}{\rho_o}\right) + E \frac{\rho}{\rho_o} \right] \quad (3)$$

$$R_D = \frac{2}{3} R_u + \frac{1}{2} R_l \quad (4)$$

$$R_D = R_u - \lambda^* \left[1 - \left(1 - \frac{W}{W^*}\right) P/P^* \right] T \quad (5)$$

Where R_D is the actual rolling radius of the wheel, R_u is the radius of the wheel without load, R_l is the radius of the loaded wheel, ρ is the actual deflection of the tire, ρ_o is the deflection of the tire at rated load, B, D, E are the design parameters of the tire, W is the vertical load on the wheel, T is the torque applied to the wheel, λ^*, W^* and P^* are the empirical factors of the tire longitudinal elasticity, load, and pressure. Studies have shown that wheel deformation contributes immensely to wheel slipping which is a

measure of the difference between rotational speed of the wheel and the translational velocity of the wheel centre as expressed in Equation 6 [22] or determined as the difference between the arc lengths in Equation 7. The actual radius (R_A) of a deformed wheel is determined using Equation 8 while the relation for coefficient of slippage [23] is given by Equation 9.

$$S = -\frac{(V - R_e w)}{V} \quad (6)$$

$$\delta_G = \frac{2\pi}{\alpha} \left(\frac{(\alpha R - 2R \sin \frac{\alpha}{2})}{\alpha R} \right) = \left(1 - \frac{2}{\alpha} \sin \frac{\alpha}{2} \right) = \left(1 - \frac{L}{\alpha R} \right) = \left(1 - \frac{R_D}{R} \right) \quad (7)$$

$$R_A = \frac{L}{\alpha} = \frac{L}{2 \text{arc} \sin \frac{L}{2R}} \quad (8)$$

$$\delta = \frac{\omega R_K - V_D}{\omega R_K} = \frac{2\pi R_K n - S_D}{2\pi R_K n} \quad (9)$$

Where V is the longitudinal speed of the wheel centre, w is the angular speed of the tire and R_e is the effective tire radius, δ is the coefficient slipping, V_D is the actual speed, ω is the angular velocity of the drive wheel, R_K is the driving wheel rolling radius, n is the number of turns made by the wheel per unit of time, S_D is the actual distance covered by the wheel for a certain number of the wheel turns, δ_G is the wheel slipping, R is the initial radius of the wheel rolling, α is the central angle limiting the chord of the wheel tire deflection, L is the length of the chord formed by the deflection of the wheel. Initial radius of the wheel is given by Equation 10 while the change in radius of the wheel caused by the load of its own weight is given by Equation 11. The stiffness of the wheel material (Equation 12) if optimum can resist changes in the radius of the wheel [24].

$$R = R_C - \Delta r = \frac{l_C}{2\pi} - \frac{(l_C - l_K)k_{DP}}{2\pi} = \frac{l_C(1 - k_{DP}) + l_K k_{DP}}{2\pi} \quad (10)$$

$$\Delta r = \frac{(l_C - l_K)k_{DP}}{2\pi} \quad (11)$$

$$k_{wheel} = (2 * \pi * f_2)^2 \left[M_T - M_T \left(\frac{f_2^2}{f_1^2} \right) \right] \quad (12)$$

Where f_l is the Maximum frequency in harmonic response, f_l is the minimum frequency in harmonic response, M_T is the mass of the wheel, R_C is the radius of the middle of the wheel tread in the Free State. Axial load (F_p) resulting from tire inflation pressure (P_o) is given by Equation 13 while the load on a unit length of the circumference of the rim flange of the rotating wheel is given by Equation 14.

$$F_p = \pi(a^2 - r_f^2)P_o \quad (13)$$

$$T_f = \frac{F_p}{4\pi r_f} = (a^2 - r_f^2) \frac{P_o}{4r_f} \quad (14)$$

where a is the design radius of the tire and r_f is the radius of the loading point on the rim flange. When the vehicle is in motion, causing the wheels to undergo a rotary motion (O) at angular velocity (Ω_z), the velocities at the axial centre of the right front wheel (O_1) are given by Equations 15a-b [25]. The slip velocities of the projection point (O_1) on the wheel-ground contact surface is given by Equations 16a-b.

$$V_{o1} = R''\Omega_z = \sqrt{\left(R'' + \frac{B}{2}\right)^2 + \left(\frac{L}{2} - S_o + C_y\right)^2} \Omega_z \quad (15a)$$

$$V_{o1x1} = R''\Omega_z \sin\alpha = \left(\frac{L}{2} - S_o + C_y\right) \Omega_z \quad (15b)$$

$$V_{t1x1} = \left(R'' + \frac{B}{2}\right)\Omega_z - r\omega_o \quad (16a)$$

$$V_{t1x1} = \left(\frac{L}{2} - S_o + C_y\right)\Omega_z \quad (16b)$$

Were the rotational angular velocity of the right wheel denoted as ω_o . The expression describing the dynamics of the angular deformation of the wheel is given by Equation 17.

$$H_\alpha \frac{d\Delta\alpha}{dt} + C_\alpha \Delta\alpha = M(\lambda) \quad (17)$$

where H_α is the energy dissipation rate of the angular deformational motion in a wheel, C_α is the angular rigidity of the wheel in the direction of the angular deformation movement therein. The angular speed of rotation and speed of translational movement of the centre of wheel mass is given by Equation 18 while The change of moment $M(\omega, V)$ of the traction point is given by Equation 19 [26]. Furthermore, the stress induced on auto wheel due to bending is given by Equation 20.

$$\Delta\alpha = \int_{t-\Delta t}^t [\omega(r_o - x_1) - V] dt \quad (18)$$

$$M(\omega, V) = C_\alpha \int_{t-\Delta t}^t \left\{ \omega - V / \left[r_o - \frac{P}{(c_o + c_\omega(1 - e^{-K\omega}))} \right] \right\} dt \quad (19)$$

$$\sigma_b = \frac{M_y}{I_c} \quad (20)$$

where C_o is the value of the radial stiffness of the wheel in rest, C_ω is the coefficient characterizing the impact of centripetal force on radial stiffness of the wheel, $K\omega$ is the coefficient characterizing the nonlinear effect of the angular speed of the wheel on its radial stiffness, P is weight of the vehicle and the wheel which influence the contact patch, V is the velocity of translational motion of the centre of the wheel mass and ω_o is the angular velocity of the wheel, M is the bending moment, y is the distance between the centroidal axis and the outer surface of

the wheel and I_c is the centroidal moment of inertia of the of the cross section about the appropriate axis.

SOLIDWORKS software, 2018 version was employed in modelling and simulating the auto wheel component presented in Figure 1. SOLIDWORKS is a solid modelling Computer Aided Design (CAD) software as well as Computer Aided Engineering (CAE) tool that runs mainly on Microsoft windows. Modelling procedure of the auto wheel commenced with 2D sketch, consisting of geometries such as arcs, points, conics, lines, splines and so on. Dimensions were added to the sketch to define the size and configuration of the geometry. Relations in the tool bar were used to define features such as parallelism, tangency, concentricity, perpendicularity among others. In the part assembly, sketches of individual parts were assembled together to form the intended solid model of the auto wheel. Views were automatically generated from the solid model; and dimensions and tolerances were added to the drawing as required. SOLIDWORKS software have been successfully employed in modelling of reciprocating piston [27], remotely controlled hydraulic Bottle Jack [28], vehicle compression springs [29], two stroke internal combustion engine [30], High Density Polyethylene Liner HDPL [31] etc. The wheel was analysed for static and dynamic loads. In the case, pressure loading, centrifugal/radial loading and vertical loading were considered. Von-mises stress, equivalent strain, resultant displacement and bending obtained from the analysis shows the maximum and minimum values induced on the auto wheel operating under the aforementioned loading conditions. The wheel was constrained appropriately and the loads were calculated based on the specifications and applied to appropriate nodes. The wheel was analysed for the calculated loading conditions and plots were obtained for each analysis performed. To fully initiate the auto wheel simulation process, the following conditions were taken cognizance of:

- i. There was a fixed support on the six bolt/stud holes, as wheels are normally installed by bolt via stud holes in vehicle axle.
- ii. A total of 7769.5 N bearing load was applied to the hub centre at Y-axis, as the hub is fixed at the central hole of the rim.
- iii. A pressure of 0.241 Mpa was considered on the tyre allocation area which acts normally at the circumferential tread and flange portion of the wheel.
- iv. Considering a tyre diameter of 550 mm, velocity of car rim was taken as 100 kmph, i.e. 965 RPM.

- v. From annexure of AIS-073 (part 2), the moment taken was 5.0969e+5 N-mm.

Figure 1 represents the auto wheel model while Figure 2 represents the mesh visualization for each material of the auto wheel model. Material properties of the auto wheel are presented in Table 1, load details for the auto wheel analysis in Table 2, fixture details for the auto wheel analysis in Table 3 and mesh information in Table 4.

3. Results and Discussion

3.1. Carbon Fibre (T300)

Carbon fibre is a fibre material of about 5-10 micrometres in diameter and is composed primarily of carbon atoms. Carbon fibre is manufactured through the process of high bonding of carbon atoms together in crystals which are more aligned to the long axis which gives the fibre a high strength to volume ratio. It has numerous advantages such as high tensile strength, high temperature tolerance, low weight, high stiffness, low thermal expansion etc. which makes carbon fibre an essential material

in the manufacturing of automotive wheel. However, it is very expensive, brittle and prone to the risk of catastrophic failure that cannot be experienced with metallic wheels. The T300 carbon fibre is a thermoset polymer matrix composite reinforced with 68% carbon fibre, and formed by laminating hot-pressed carbon fibre prepreg. Having developed the auto wheel model presented earlier in Figure 1, T300 carbon fibre was applied as the wheel material and simulated to obtain multiple profiles as shown in Figure 3a-f.

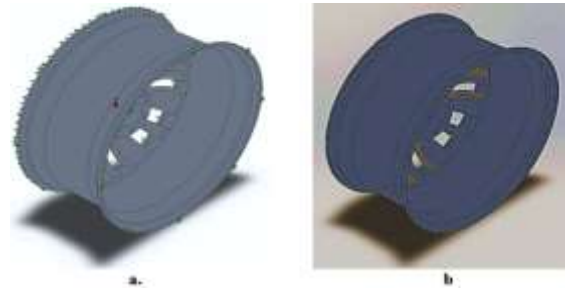


Figure 1. Auto wheel model analysed in this study

Table 1. Material properties of auto wheel (model)

Name	Carbon fiber (T300)	Cast Alloy Steel	Aluminium (2014-T6)	Magnesium Alloy
Model type	Linear Elastic Isotropic	Linear Elastic Isotropic	Linear Elastic Isotropic	Linear Elastic Isotropic
Yield strength	3.44e+008 N/m ²	4.41e+008 N/m ²	4.15e+008 N/m ²	6.24+008 N/m ²
Tensile strength	1.86e+009 N/m ²	4.48e+008 N/m ²	4.7e+008 N/m ²	4.48e+008 N/m ²
Elastic modulus	1.35e+011 N/m ²	1.9e+011 N/m ²	7.24e+010 N/m ²	4.5e+010 N/m ²
Poisson's ratio	0.3	0.26	0.33	0.35
Mass density	1700 kg/m ³	7300 kg/m ³	2800 kg/m ³	1760 kg/m ³
Shear modulus	9.8e+007 N/m ²	7.8e+010 N/m ²	2.8e+010 N/m ²	1.7e+010 N/m ²
Thermal expansion coefficient	1.5e-005 /Kelvin	1.5e-005 /Kelvin	2.3e-005 /Kelvin	2.5e-005 /Kelvin

Table 2. Load details for the auto wheel analysis

Load name	Load Image	Load Details	
Pressure-1		Entities	9 face(s)
		Type	Normal to selected face
		Value	255.692
		Units	N/m ²
		Phase Angle	0
		Units	deg
Gravity-1		Reference	Top Plane
		Values	0 0 -9.81
		Units	m/s ²

Table 3. Fixture details for the auto wheel analysis



Fixture name	Fixture Image	Fixture Details		
Fixed Hinge-2		Entities	6 face(s)	
		Type	Fixed Hinge	
Resultant Forces				
Components	X	Y	Z	Resultant
Reaction force(N)	2.88696	22.2569	0.028139	22.4434
Reaction Moment (N.m)	0	0	0	0
Fixed-1		Entities	2 face(s)	
		Type	Fixed Geometry	
Resultant Forces				
Components	X	Y	Z	Resultant
Reaction force (N)	-2.88833	42.2323	-0.0292426	42.331
Reaction Moment (N.m)	0	0	0	0

Table 4. Mesh information for the auto wheel analysis

Mesh details for the wheel rim analysis		Specification of proposed car wheel rim	
Mesh type	Solid Mesh	Specification	Value
Mesher Used	Blended curvature-based mesh	Bolt circle diameter	68 mm
Jacobian points	4 Points	Width of the rim	140 mm
Maximum element size	26.4766 mm	Diameter of the rim	355 mm
Minimum element size	5.29532 mm	Offset	57 mm
Mesh Quality Plot	High	Central hole diameter	40 mm
Total Nodes	56016	Rim thickness	7 mm
Total Elements	31880	Hole circle diameter	15 mm
Maximum Aspect Ratio	421.11	Number of stud hole	5 No's
% of elements with Aspect Ratio < 3	83		
% of elements with Aspect Ratio > 10	2.58		
% of distorted elements (Jacobian)	0		
Time to complete mesh (hh:mm:ss):	00:02:28		

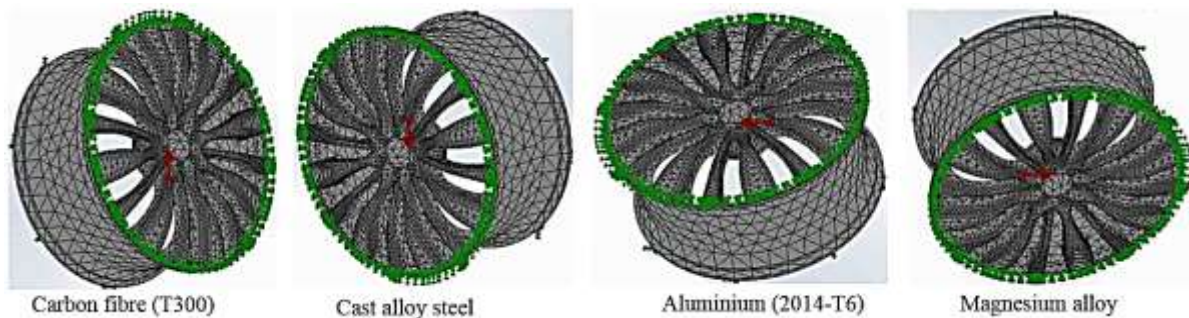


Figure 2. Mesh visualization for each material of the auto wheel model

3.2. Cast alloy steel

Cast steel is a ferrous alloy with maximum carbon content of approximately 0.75% and other elements including silicon, manganese, iron, aluminium, zirconium etc. It has high resistance to impact

cracks, high strength, toughness, can withstand abrasion and high loading deformation due to high carbon content and inexpensive compared to carbon fibre, aluminium and magnesium alloy. The aforementioned properties makes it suitable for auto

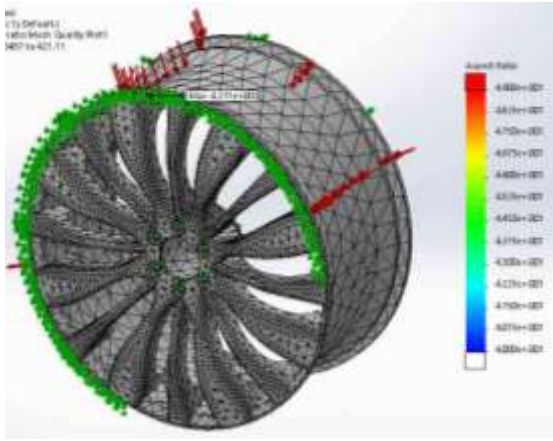


Figure 3a. Aspect ratio

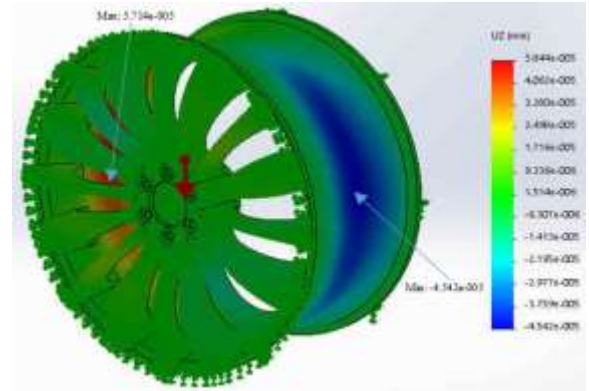


Figure 3e. Radial displacement

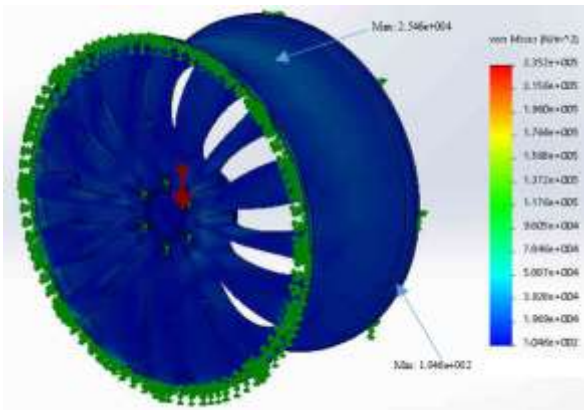


Figure 3b. Static nodal stress

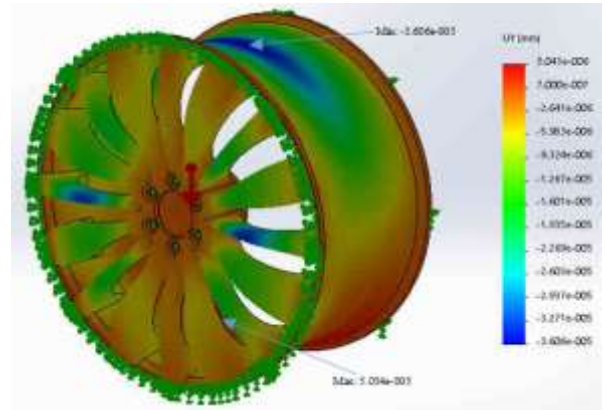


Figure 3f. Bending

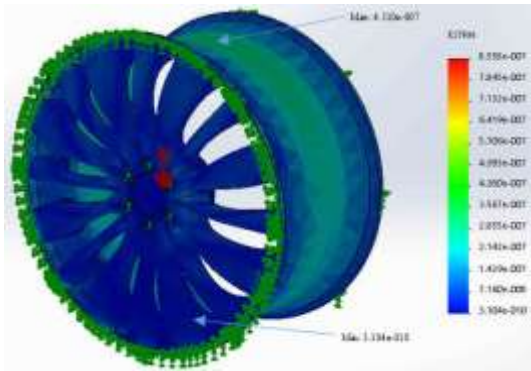


Figure 3c. Equivalent Static strain

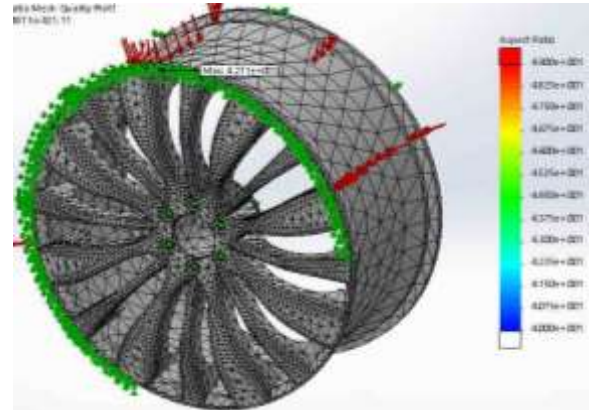


Figure 4a. Aspect ratio

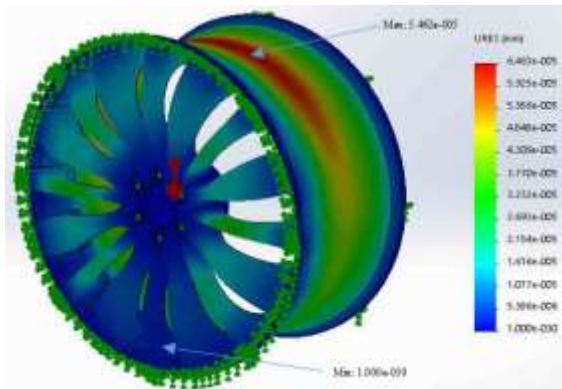


Figure 3d. Static displacement

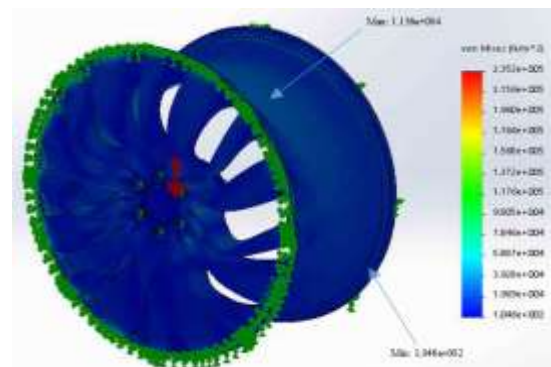


Figure 4b. Static nodal stress

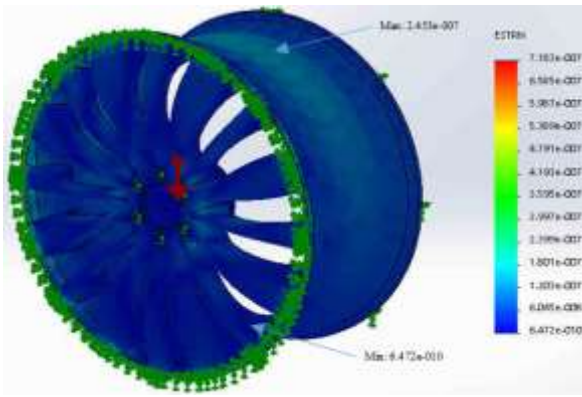


Figure 4c. Equivalent static strain

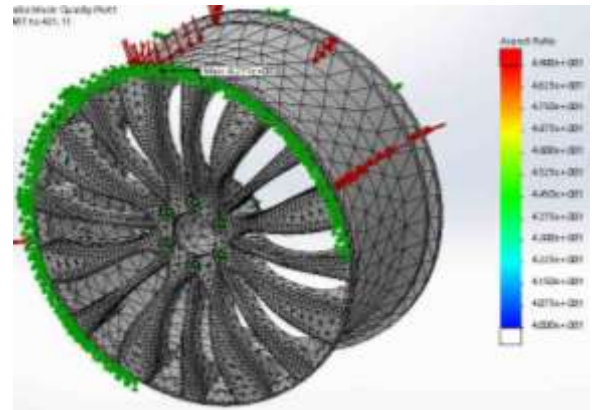


Figure 5a. Aspect ratio

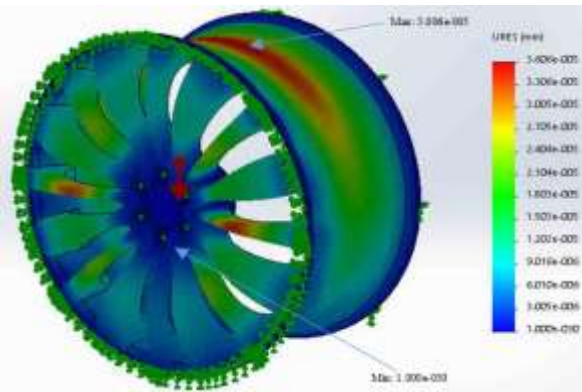


Figure 4d. Static displacement

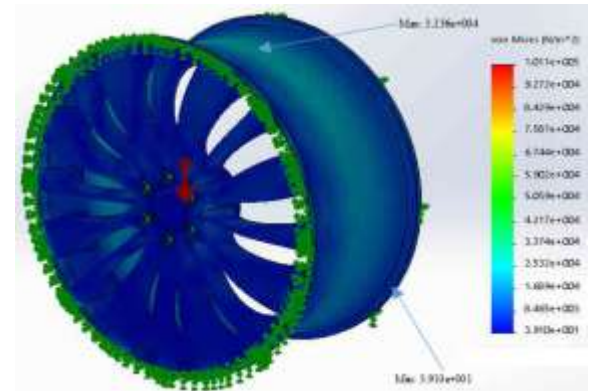


Figure 5b. Static nodal stress

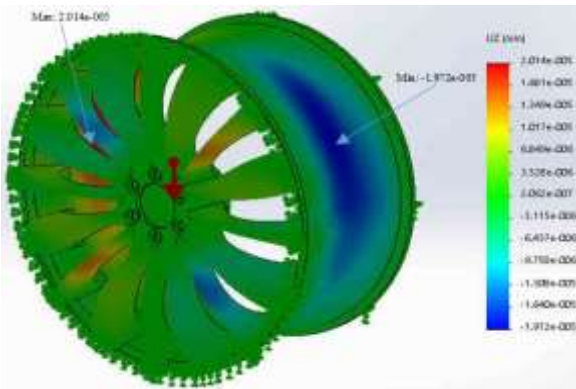


Figure 4e. Radial displacement

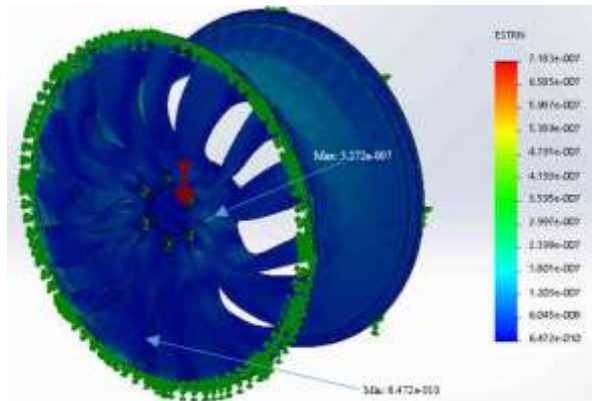


Figure 5c. Equivalent static strain

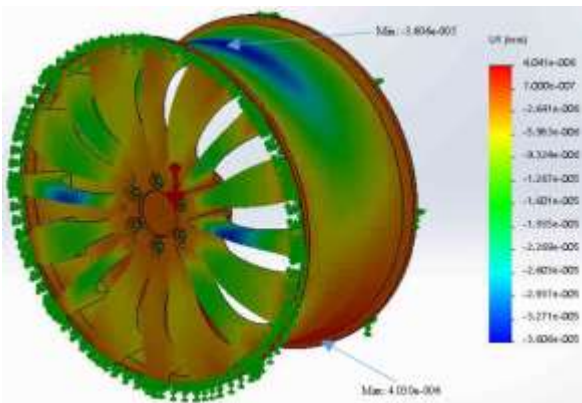


Figure 4f. Bending

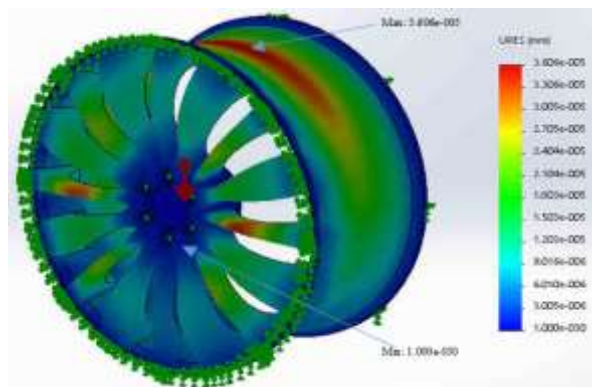


Figure 5d. Static displacement

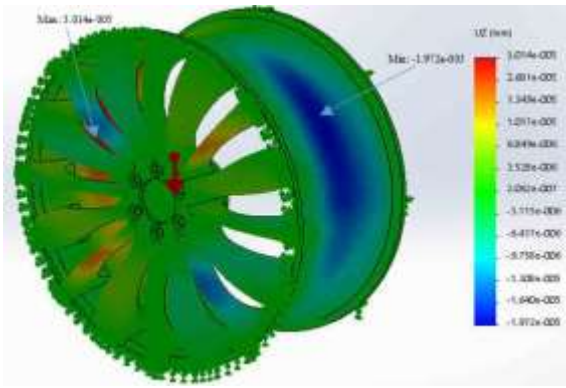


Figure 5e. Radial displacement

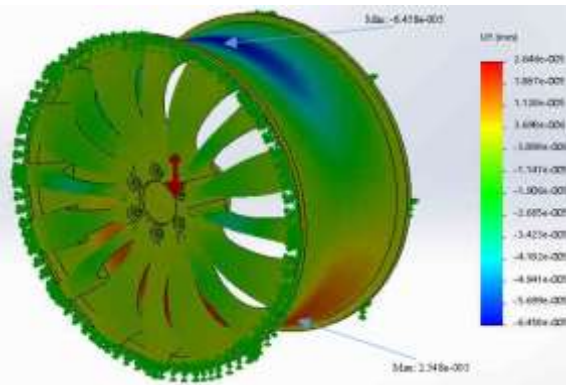


Figure 5f. Bending

wheel application but it has a major disadvantage which is the unit weight. Having developed the auto wheel model presented earlier in Figure 1, cast alloy steel was applied as the wheel material and simulated to obtain multiple profiles as shown in Figure 4a-f.

3.3. Aluminium 2014-T6

2014-T6 aluminium is 2014 aluminium in the T6 temper which is achieved by solution heat-treatment and artificial age-hardening treatment to obtain the standard mechanical required. As one of the strongest aluminium alloy, aluminium 2014-T6 is a precipitation hardening alloy with high electrical conductivity, low density, ductile, excellent machinability, cost effective and fair corrosion resistant property. It is used in applications that require high strength/hardness as well as elevated temperature such as auto wheel, heavy duty forgings, tangs, automotive frame etc. However, it contains high amount of copper, making it less corrosion-resistance. Therefore, requires anti-corrosion treatment if exposed to corrosive environment. Having developed the auto wheel model presented earlier in Figure 1, 2014-T6

aluminium was applied as the wheel material and simulated to obtain multiple profiles as shown in Figure 5a-f.

3.4. Magnesium Alloy

Magnesium alloy is known for being the lightest structural alloy. It is formed from a mixture of magnesium (the lightest structural metal) and other metals elements (known as alloying elements) usually manganese, zinc, aluminium, copper, silicon etc. to improve the mechanical properties [32]. Magnesium alloy has a number of merits such as low specific gravity with satisfactory strength, higher specific modulus, withstand greater loading per unit weight, low density which makes it suitable for wheel-rims in automobiles. The strength of magnesium alloy however depreciates at elevated temperature. Therefore, temperature as low as 200 °F (93 °C) yields considerable reduction in the yield strength of magnesium alloy [33]. Having developed the auto wheel model presented earlier in Figure 1, magnesium alloy was applied as the wheel material and simulated

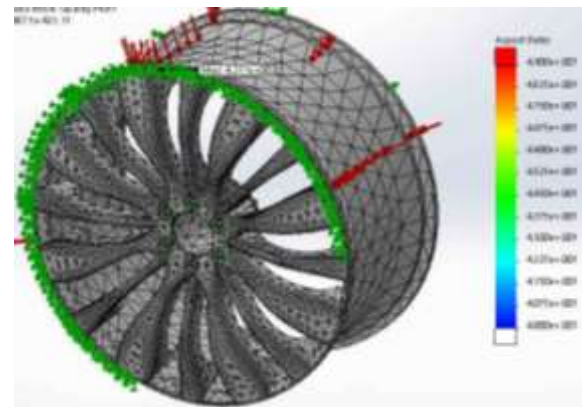


Figure 6a. Aspect ratio

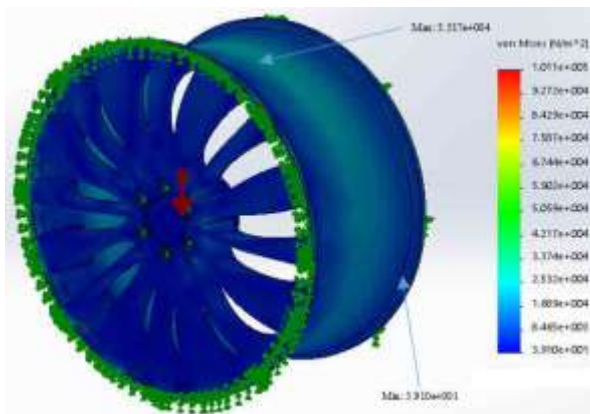


Figure 6b. Static nodal stress

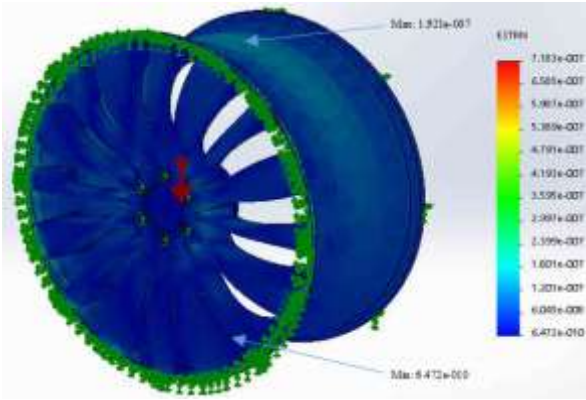


Figure 6c. Equivalent static strain

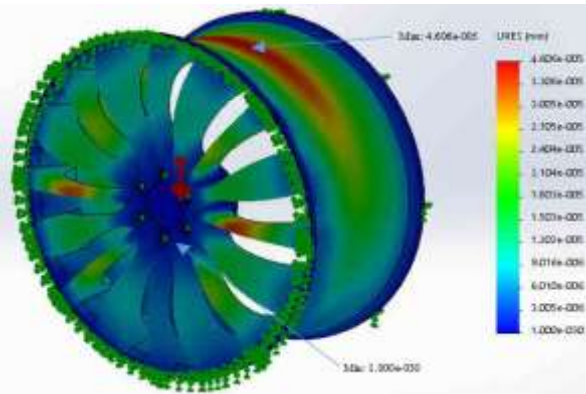


Figure 6d. Static displacement

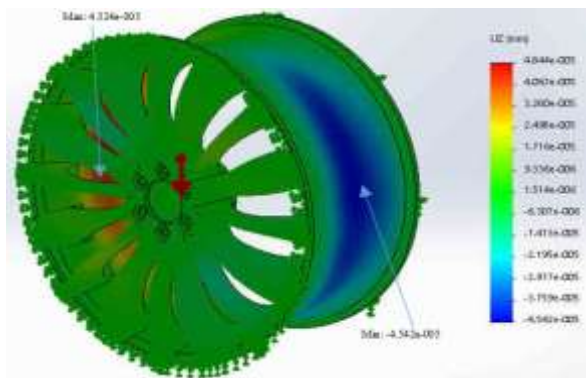


Figure 6e. Radial displacement

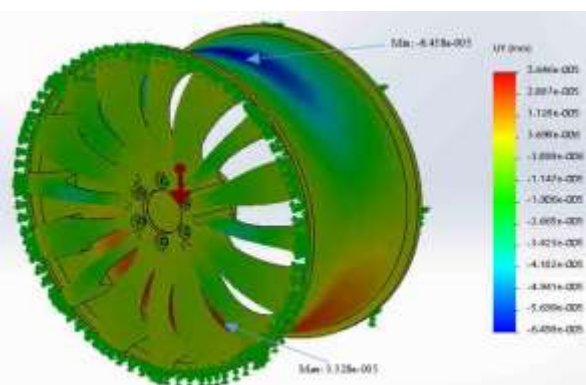


Figure 6f. Bending

to obtain multiple profiles as shown in Figure 6a-f. The deflected auto wheel models obtained from the finite element simulation profiles are characterized by different colors corresponding with the simulation results shown on the color bands. Areas with high stress concentration, high resultant displacement, high equivalent strain as well as high bending stress indicates unsafe zones which are prone to high level deformation and vice versa [34, 35], and can be identified using the color band or legend on the simulated plots presented in Figures 3-6. Red color which is at the top of the color band indicates the area with maximum stress, resultant displacement, equivalent strain and bending stress concentration on the auto wheel component. This is followed by orange color, light green color, green color and so on. On the other hand, royal blue which is at the bottom of the color band indicates safe zones as well as the areas with minimum stress concentration on the wheel component. Sky blue indicates the stress level at which the shaft material begins to respond to the applied load, aqua (SVG) blue indicates further stress level from sky blue color [36, 37]. Figure 7 shows the maximum Von-mises stress derived from each of the auto wheel material employed in this study. Results shown on the plot in Figure 7 reveals that carbon fibre (T300) had the highest static nodal stress ($5.35E+04 \text{ N/m}^2$), followed by magnesium alloy ($4.22E+04 \text{ N/m}^2$), 2014-T6 aluminium alloy ($3.14E+04 \text{ N/m}^2$) and then cast alloy steel as the least ($1.14E+04 \text{ N/m}^2$). This implies that auto wheel material with maximum static nodal stress will fail first before the one with minimum static nodal stress. Considering von-Mises failure theory, material component is said to be in a state of failure if the von-Mises stress exceeds the material yield strength, but if the von-Mises stress value is lower than the material's yield strength, the material is considered to be safe [38, 39]. Considering the maximum von-Mises stresses and yield strength obtained from each auto wheel simulated profile, it can be observed that the maximum von-mises stress values for the four (4) wheel materials were below their yield strength, indicating that all the for materials in this study considered are good choice of materials that can withstand the in-service loading condition of an auto wheel application without untimely failure. Figure 8 shows the maximum resultant static strain derived from each of the auto wheel material employed in this study.

Results shown on the plots in Figure 8 reveals that magnesium alloy had the highest resultant static strain ($3.31E-07$), followed by 2014-T6 aluminium alloy ($3.17E-07$), cast alloy steel ($2.45E-07$) and then carbon fibre (T300) as the least ($1.92E-07$). From the

maximum strain obtained from each profile, the values are insignificant, implying that the rate of strain elongation on the auto wheel component due to static and dynamic loads is within tolerable level that will not result in catastrophic failure. The low static resultant strain exhibited by carbon fibre is due to the high stiffness and high tensile strength of the material. Strain is the ratio of change in deformation undergone by an object in response to the applied load or force to its original length [40]. The static or dynamic loads may take the form of compression or stretching which incite stresses within the molecular bonding of the material, causing the atomic bonding to detach from one another. Strain elongation on the wheel can also occur due to thermal expansion coefficient which is the equivalent strain divided by the change in temperature of the wheel in motion. This can cause increase in strain along the bonded area within the atoms in the metal lattice as the auto wheel temperature increases during service condition. Figure 9 shows the maximum static displacement derived from each of the auto wheel material employed in this study.

Results shown on the plot in Figure 9 reveals that carbon fibre (T300) had the highest static displacement ($5.46E-05$ mm), followed by magnesium alloy ($4.61E-05$ mm), 2014-T6 aluminium alloy ($3.61E-05$ mm) and then cast alloy steel as the least ($3.01E-05$). Figure 10 shows the maximum radial displacement derived from each of the auto wheel material employed in this study. Results shown on the plots reveal that carbon fibre (T300) had the highest static displacement ($5.71E-05$ mm), followed by magnesium alloy ($4.32E-05$

mm), 2014-T6 aluminium alloy ($3.01E-05$ mm) and then cast alloy steel as the least ($2.01E-05$). Displacement is a vector quantity that refers to the extent at which a body deviates from its original place or length. It is also the overall change in position of an object due to external forces or loads acting on them, which in this case is the static and dynamic loads acting on the auto wheel component. The change in position or deviation from the original length is a property that relates to the geometric distortion or structural deformation of the wheel from its original geometry. Hence, the static and dynamic loads acting on the auto wheel component are responsible for the static and radial displacements discussed in this paper.

Figure 11 shows the maximum bending deformation derived from each of the auto wheel material employed in this study. Results shown on the plot in Figure 11 reveals that carbon fibre (T300) had the highest bending deformation ($5.03E-05$ mm), followed by magnesium alloy ($3.33E-05$ mm), 2014-T6 aluminium alloy ($2.55E-05$ mm) and then cast alloy steel as the least ($4.03E-06$). Bending deformation also known as flexural stress is a more specific form of normal stress induced on a structurally loaded member like the auto wheel subjected to tensile or compressive forces. In other words, normal stress is a result of an external load acting perpendicularly to longitudinal axis of the wheel component. The exact value of the normal force (curb weight of the car) acting on the wheel component which eventually results in bending deformation is simply the force divided by the cross sectional area of the auto wheel.

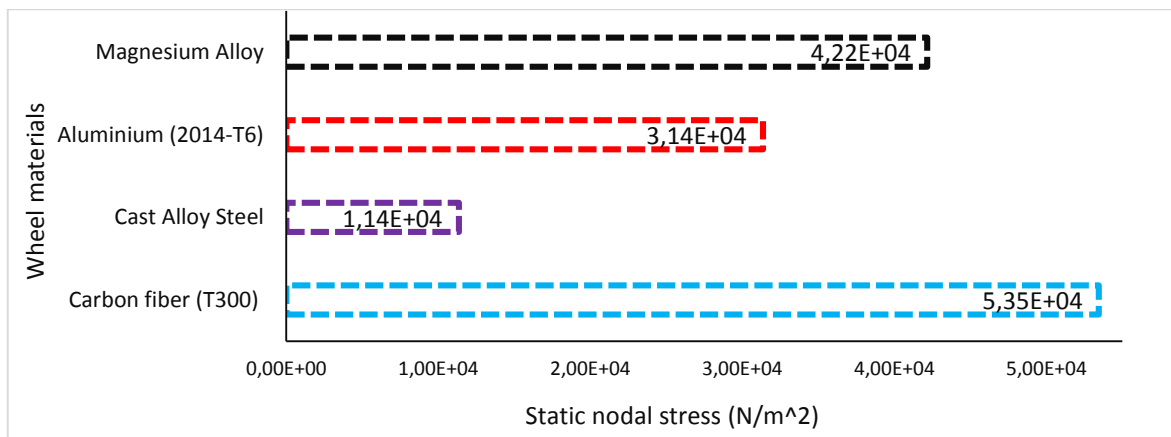


Figure 7. Maximum static nodal stress (von-mises) derived from each wheel material

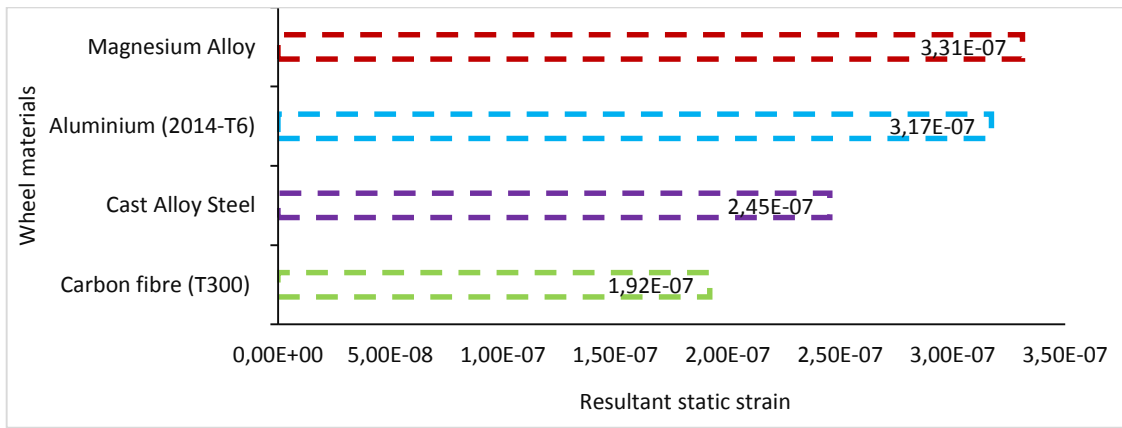


Figure 8. Maximum resultant static strain derived from each wheel material

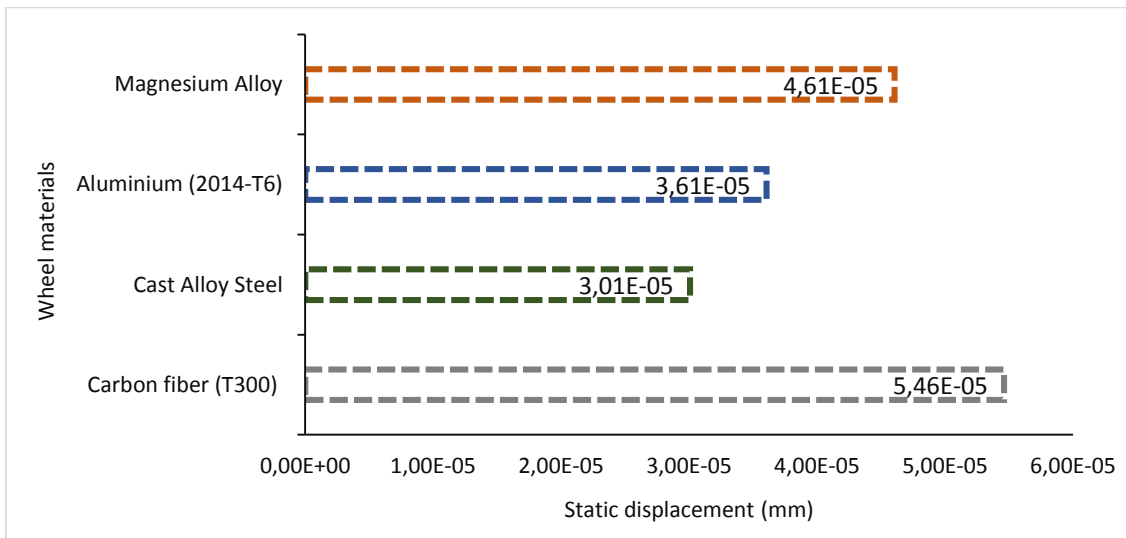


Figure 9. Maximum static displacement derived from each wheel material

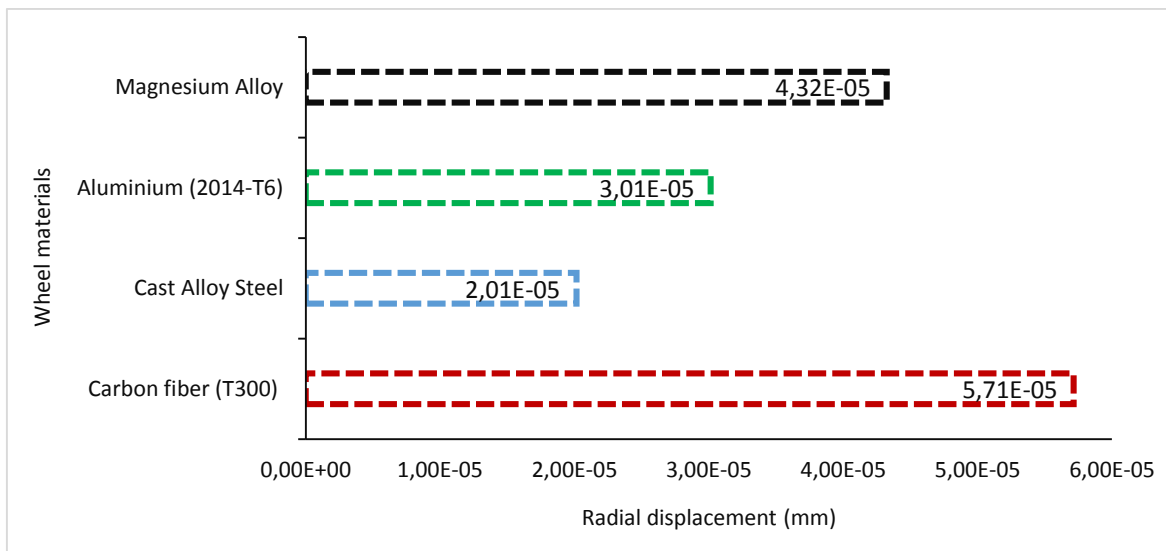


Figure 10. Maximum radial displacement derived from each wheel material

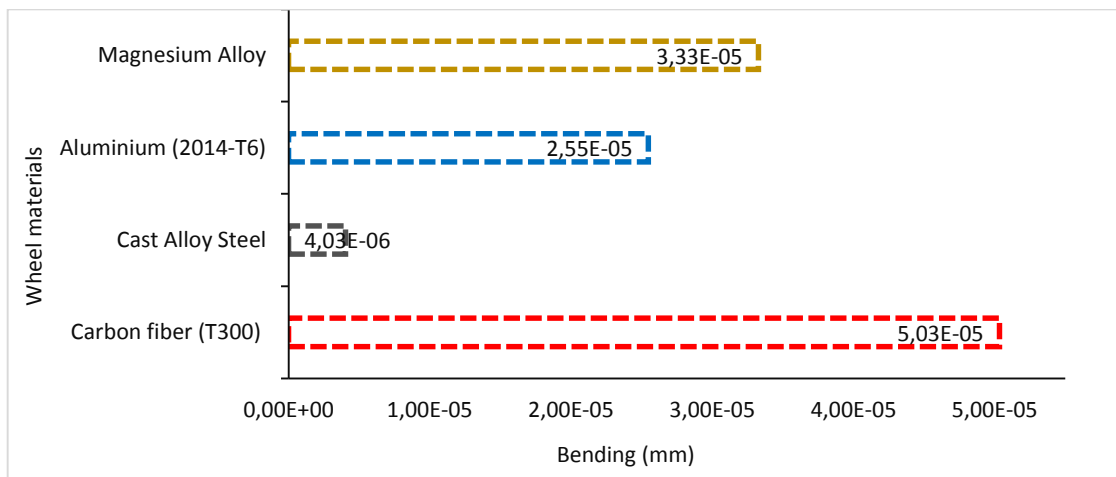


Figure 11. Maximum bending derived from each wheel material

4. Conclusion

The study reveals that Steel wheels (cast alloy steel) in terms of mass are heavier than aluminium (2014-T6), magnesium (alloy) and carbon fibre (T300) based wheels while wheels produced from carbon fibre are the lightest and aluminium wheels are slightly heavier than magnesium wheels. Weight of the wheel can be referred to unsprung weight particularly when it is denser which is not being cushioned by the suspension springs, and cast alloy steel is a clear example in this case. Acceleration and agility of the car is dampened by the excess weight of the wheel, lowers the vehicle's centre of gravity and causes it to drive sluggishly while also consuming more fuel. However, while wheels designed with carbon fibre are very expensive, steel wheels in terms of cost are the cheapest and inexpensive to replace if extremely damaged while wheels produced from magnesium alloy are cheaper than their aluminium counterpart. In terms of strength and resistance against in-service defects like bending, stress-strain deformation as well as static displacement, steel wheels are better choices followed by aluminium wheels and magnesium wheels. However, carbon fibre (T300) wheels tend to be brittle, cracks more easily and cannot withstand roads with pot holes and rough patches, whereas, steel, aluminium and magnesium wheels tend to bend at extremely high impact force and hardly cracks when impacted by road (particularly steel wheels) due to their toughness and somewhat ductile nature. In terms of thermal expansion, magnesium wheel is not a good choice of material when high temperature or long distance drive that will end up raising the auto wheel temperature is involved. In this case, carbon fibre is the best choice of auto wheel material among the four auto wheel materials reported in this study. This is seconded by steel

wheel and then aluminium wheel. When considering availability, the wide range of steel and aluminium wheels available for different purposes are easy to find irrespective of the size or style. In terms of rust/corrosion, wheels produced from carbon fibre are better choices followed by aluminium and the magnesium, but as long as the paint layer in steel wheels remain intact, steel wheel can hardly rust. Hence, the choice of auto wheel depends on the user's requirement. For example, steel wheel is the right choice when an inexpensive, strong, tough and rugged wheel is required (particularly in rough terrains) and vice versa.

Author Statements:

- The authors declare that they have equal right on this paper.
- The authors declare that they have no known competing financial interests or personal relationships that could have appeared to influence the work reported in this paper
- The authors declare that they have nobody or no-company to acknowledge.

References

- [1] Thakare, R. B. "Stress analysis in wheel rim by using dynamic cornering fatigue test under different conditions". International journal of Advance Research and Innovative Ideas in Education, 3, 2(2017), 4863-4868.
- [2] Nirala, S. K., Shankar, S., Sathishkumar, D., Kavivalluvan, V., Sivakumar, P. "Carbon fiber composites: A solution for light weight dynamic components of AFVs". Defence Science Journal, 67, 4(2017), 420-427.
- [3] Natrayan, L., Santhakumar, P., Kumar, P. D., Raj, R. M., Mohandass, R. (2016) "Design and Comparative Analysis of Old and New Model Car Wheel Rims

- with Various Materials.” IETE Journal for Research, 2, 2(2016), 69-73.
- [4] Nair, A., Kawade, S., Dias, B., George, I., Bhandarkar, D. K. “Performance Enhancement and Analysis By Reducing Weight of Unsprung Mass of Formula Student Racing Car”. International Journal of Mechanical and Production Engineering, 6, 6(2018), 38-42.
- [5] Dinesh K. M., Narendra M. P., Purna C. S. B., Touseef, A. M. “Static analysis of wheel rim using CATIA and ANSYS16.0. International Research Journal of Engineering and Technology, 3, 7(2016), 2256-2261.
- [6] Bao, Y., Zhao, X. “Research of lightweight composite automobile wheel”. World Journal of Engineering Technology, 5(2017) 675-683.
- [7] Bisht, P. S., Awasthi, A. “Design and Analysis of Composite and Al Alloy Wheel Rim”. Advances in Materials Engineering and Manufacturing Processes, 5(2020), 15-29.
- [8] Blasco, J., Valero, F., Besa, A. and Rubio, F. “Design of a Dynamometric Wheel Rim”. Mechanisms and Machine Science, 17(2014), 243-250.
- [9] Babu, M., Hariharan, V. S. “Modelling and analysis of automotive wheel rim”. International Journal of Innovative Research in Science, Engineering and Technology, 5, 4(2016), 6192-99.
- [10] Panda, S. S., Gurung, J., Chatterjee, U. K., Sahoo S. “Modelling-and-Fatigue-Analysis-of- Automotive-Wheel-Rim”. International Journal of Engineering Sciences and Research Technology, 5, 4(2016), 428-435.
- [11] Prasad, T. D., Krishnaiah, T., Iliyas, J. M., Reddy, M. J. “A Review on Modelling and Analysis of Car Wheel Rim using CATIA and ANSYS”. International Journal of Innovative Science and Modern Engineering, 2, 6(2014), 1-5.
- [12] Venkateswarlu, G., Sharma, M. “Design and Analysis of Alloy Wheel with Different Alloys”. International Journal of Advance Research in Science and Engineering, 6, 10(2017), 2488-2495.
- [13] Kumar, D. S., Jayakumar, V., Majeed, S. “Modal Analysis and Design Optimization of Automotive Wheel Rim”. Journal of Chemical and Pharmaceutical Sciences, 10, 1(2017), 667-669.
- [14] Burande, D. H., Kazi, T. N. “Fatigue Analysis of Alloy Wheel for Passenger Car under Radial Load”. International Journal of Engineering Research and General Science 4, 2(2016), 26-36.
- [15] Sekhar, V., Mouli, A. C. “Design and Performance Analysis of Alloy Wheels using CATIA ANSYS Modelling Tool”. International Journal of Scientific Engineering and Technology Research, 3, 43(2014), 8789-8793.
- [16] Ikpe, A. E., Owunna, I., Egunilo, P. O. “Comparison of Aluminium Wheel to Steel Wheel in Relation to Weight and Fuel Consumption (Energy) in Automobiles”. Industrial and Systems Engineering, 1, 1(2016), 1-9.
- [17] Stearns J., Srivatsan T., Gao, X., Lam, P. “Understanding the Influence of Pressure and Radial Loads on Stress and Displacement Response of a Rotating Body: The Automobile Wheel”. International Journal of Rotating Machinery, 60193(2006), 1-8.
- [18] Golub G. A., Chuba V. V., Marus O. A. “Determination of Rolling Radius of Self-Propelled Machines’ Wheels”. INMATEH-Agricultural Engineering, 57, 1(2019), 81-90.
- [19] Pauwelussen, J. P., Dalhuijsen, W., Merts, M. “Tyre dynamics, tyre as a vehicle component Part 1: Tyre Handling Performance.” Virtual Education in Rubber Technology, HAN University, Netherlands, 2007.
- [20] Jazar R. N. “Vehicle dynamics: Theory and application, 3rd Edition.” Switzerland, Springer, 2017.
- [21] Wilson T., Siero M., Kopchick C., Vantsevich V. “Terrain Truck: Control of Wheel Rotational Velocities and Tire Slippages”. SAE Technical Paper 2011-01-2157, 2011.
- [22] Miller, S. L., Youngberg, B., Millie, A., Schweizer, P., Gerdes, J. C. “Calculating Longitudinal Wheel Slip and Tire Parameters Using GPS Velocity”. Proceedings of the American Control Conference, Arlington, VA, June 25-27, (2001), 1800-1805.
- [23] Smieszek, M., Dobrzanska, M., Dobrzanski, P. “The impact of load on the wheel rolling radius and slip in a small mobile platform”. Autonomous Robots, 43(2019), 2095-2109.
- [24] Undru, S., Reddy, P. P. “Design and Analysis of Aluminium Alloy Wheel”. International Journal of Engineering Research and Application, 7, 3(2017), 57-65.
- [25] Ren, F., Li, L., Jiang, Z., Song, T., Gong, Z., Shi, Y., Liu, B. “Analysis on Wheel-Ground Contact Load Characteristics of Unmanned Off-road Vehicles”. Journal of Engineering Science and Technology Review 10, 3(2017), 97-103.
- [26] Lapshin, V. P., Turkin, I. A. “Modelling Tractive Effort Torque of Wheel in Deformation Movements of Pneumatic Tire Wheel”. Procedia Engineering, 206(2017), 594-599.
- [27] Owunna, I. B., Ikpe, A. E. “Design Analysis of Reciprocating Piston for Single Cylinder Internal Combustion Engine”. International Journal of Automotive Science and Technology, 4, 2(2020), 30-39.
- [28] Ikpe, A. E., Owunna, I. B. “Design of Remotely Controlled Hydraulic Bottle Jack for Automobile Applications”. International Journal of Engineering Research and Development, 11, 1(2019), 124-134.
- [29] Ikpe, A. E., Owunna, I. “Design of Vehicle Compression Springs for Optimum Performance in their Service Condition”. International Journal of Engineering Research in Africa, 33(2017), 22-34.
- [30] Ikpe, A. E., Owunna, I. B. “A 3D Modelling of the In-Cylinder Combustion Dynamics of Two Stroke Internal Combustion Engine in its Service Condition”. Nigerian Journal of Technology, 39, 1(2020), 161-172.
- [31] Ikpe, A. E., Ndon, A. E., Adoh, A. U. “Modelling and Simulation of High Density Polyethylene Liner

- Installation in Engineered Landfill for Optimum Performance. *Journal of Applied Science and Environmental Management*, 23, 3(2019), 449-456.
- [32] Trang, T. T., Zhang, J. H., Kim, J. H., Zargar, A., Hwang, J. H., Suh, B., Kim, N. J. "Designing a Magnesium Alloy with High Strength and High Formability". *Nature Communication*, 9(2018), 1-6.
- [33] Mo, J. "Current Development of Creep-resistant Magnesium Cast Alloy: A Review". *Materials and Design*, 155(2018), 422-442.
- [34] Ikpe, A. E., Orhororo, E. K., Gobir, A. "Design and Reinforcement of a B-Pillar for Occupants Safety in Conventional Vehicle Applications". *International Journal of Mathematical, Engineering and Management Sciences*, 2, 1(2017), 37-52.
- [35] Ikpe, A. E., Owunna, I. B., Satope, P. "Design optimization of a B-pillar for crashworthiness of vehicle side impact". *Journal of Mechanical Engineering and Sciences*, 11, 2(2017), 2693-2710.
- [36] Ikpe, A. E., Owunna, I. "Design of Vehicle Compression Springs for Optimum Performance in their Service Condition". *International Journal of Engineering Research in Africa*, 33(2017), 22-34.
- [37] Ikpe, A. E., Efe-Ononeme, O. E., Ariavie, G. O. "Thermo-Structural Analysis of First Stage Gas Turbine Rotor Blade Materials for Optimum Service Performance". *International Journal of Engineering and Applied Sciences*, 10, 2(2018), 118-130.
- [38] Ikpe, A. E., Owunna, I. B. "Design of Remotely Controlled Hydraulic Bottle Jack for Automobile Applications". *International Journal of Engineering Research and Development*, 11, 1(2019), 124-134.
- [39] Owunna, I. B., Ikpe, A. E. "Design Analysis of Reciprocating Piston for Single Cylinder Internal Combustion Engine". *International Journal of Automotive Science and Technology*, 4, 2(2020), 30-39.
- [40] Ikpe, A. E., Owunna, I., Ebulilo, P. O. "Determining the Accuracy of Finite Element Analysis when Compared to Experimental Approach for Measuring Stress and Strain on a Connecting Rod Subjected to Variable Loads". *Journal of Robotics, Computer Vision and Graphics*, 1, 1(2016), 12-20.